Organic Geochemistry 47 (2012) 120–131

Contents lists available at SciVerse ScienceDirect

Organic Geochemistry

journal homepage: www.elsevier.com/locate/orggeochem

Effect of organic-matter type and thermal maturity on methane adsorption in shale-gas systems

Tongwei Zhang [a,*], Geoffrey S. Ellis [b], Stephen C. Ruppel [a], Kitty Milliken [a], Rongsheng Yang [a]

[a] Bureau of Economic Geology, The University of Texas at Austin, United States
[b] US Geological Survey, Denver, CO, United States

ARTICLE INFO

Article history:
Received 14 October 2011
Received in revised form 27 March 2012
Accepted 28 March 2012
Available online 5 April 2012

ABSTRACT

A series of methane (CH_4) adsorption experiments on bulk organic rich shales and their isolated kerogens were conducted at 35 °C, 50 °C and 65 °C and CH_4 pressure of up to 15 MPa under dry conditions. Samples from the Eocene Green River Formation, Devonian–Mississippian Woodford Shale and Upper Cretaceous Cameo coal were studied to examine how differences in organic matter type affect natural gas adsorption. Vitrinite reflectance values of these samples ranged from 0.56–0.58 %R_o. In addition, thermal maturity effects were determined on three Mississippian Barnett Shale samples with measured vitrinite reflectance values of 0.58, 0.81 and 2.01 %R_o.

For all bulk and isolated kerogen samples, the total amount of methane adsorbed was directly proportional to the total organic carbon (TOC) content of the sample and the average maximum amount of gas sorption was 1.36 mmol of methane per gram of TOC. These results indicate that sorption on organic matter plays a critical role in shale-gas storage. Under the experimental conditions, differences in thermal maturity showed no significant effect on the total amount of gas sorbed. Experimental sorption isotherms could be fitted with good accuracy by the Langmuir function by adjusting the Langmuir pressure (P_L) and maximum sorption capacity (Γ_{max}). The lowest maturity sample (%R_o = 0.56) displayed a Langmuir pressure (P_L) of 5.15 MPa, significantly larger than the 2.33 MPa observed for the highest maturity (%R_o > 2.01) sample at 50 °C.

The value of the Langmuir pressure (P_L) changes with kerogen type in the following sequence: type I > type II > type III. The thermodynamic parameters of CH_4 adsorption on organic rich shales were determined based on the experimental CH_4 isotherms. For the adsorption of CH_4 on organic rich shales and their isolated kerogen, the heat of adsorption (q) and the standard entropy (Δs^0) range from 7.3–28.0 kJ/mol and from −36.2 to −92.2 J/mol/K, respectively.

1. Introduction

Organic rich shales have received renewed research focus the past few years because of their emergence as hydrocarbon reservoirs (Montgomery et al., 2005; Loucks and Ruppel, 2007; Rowe et al., 2008; Ruppel and Loucks, 2008). Research on mudrock attributes has increased dramatically since shale-gas systems have become commercial hydrocarbon production targets (Jarvie et al., 2007; Rowe et al., 2008; Loucks et al., 2009). Shale gases are unconventional gas systems in which the shale is both the source of, and the reservoir for, methane, which is derived from the organic matter within the shale through biogenic and/or thermogenic processes (Hill et al., 2007; Strapoc et al., 2010). Natural gas stored in shale-gas reservoirs is thought to exist in one of three forms: (1) free gas in pores and fractures, (2) sorbed gas in organic matter and on inorganic minerals, and (3) dissolved gas in oil and water. Understanding the relative proportions of gas stored in these different forms is critical to an accurate assessment of shale-gas resources and design of effective production strategies.

Gas-in-place (GIP) is crucial to shale-gas resource assessment, but estimation of gas volumes in shales is difficult (Ambrose et al., 2010). GIP is controlled by gas generation, gas preservation and rock petrophysical properties (porosity and permeability). Most pores in some shales are located in organic matter, whereas in other shale pores are largely associated with mineral grains (Reed and Loucks, 2007; Loucks et al., 2009; Sondergeld et al., 2010). The presence of organic matter in shales lowers density, increases porosity, provides the source of gas, imparts anisotropy, alters wettability and facilitates adsorption. Recent work on siliceous mudstones from the Mississippian Barnett Shale of the Fort Worth Basin, Texas, shows that the pores in these rocks are dominantly nanopores, ranging from 5–750 nm and most pores are in grains of organic matter as intraparticle pores, with a median nanopore size of approximately 100 nm (Loucks et al., 2009; Milliken et al., 2012). Reported porosity of kerogen with SEM images is around

* Corresponding author. Tel.: +1 512 232 1496.
E-mail address: tongwei.zhang@beg.utexas.edu (T. Zhang).

0146-6380/$ - see front matter © 2012 Elsevier Ltd. All rights reserved.
http://dx.doi.org/10.1016/j.orggeochem.2012.03.012

20–25% at a thermal maturity of about 1.6 %R_o (Loucks et al., 2009; Wang and Reed, 2009) and reported porosity of kerogen by Sondergeld et al. (2010) reaches as high as 50%. Significant GIP appears to be associated with interconnected large nanopores within the organic material (Ambrose et al., 2010, 2011). The finely dispersed, porous organic material (kerogen) in shales plays an important role in gas storage.

A strong positive correlation between total organic carbon (TOC) and total gas content from the canister desorption of fresh cores in Owen and Pike Counties, Indiana (Devonian–Mississippian New Albany Shale, eastern Illinois Basin), shows that organic matter content is primarily responsible for total GIP in the New Albany Shale (Strapoc et al., 2010). A general positive correlation of CH_4 sorption capacity with TOC in shales has been observed in previous studies (Lu et al., 1995; Ross and Bustin, 2007; Cui et al., 2009). Methane sorption in Devonian–Mississippian shales in the Western Canada Sedimentary Basin (WCSB) linearly increases with TOC and micropore volume (*micropore* refers to <2 nm pores characterized by low pressure CO_2 adsorption analysis), indicating that microporosity associated with the organic fraction is a primary control on CH_4 sorption (Ross and Bustin, 2009). However, thermally immature Jurassic shales in the WCSB are organically richer than Devonian–Mississippian shales, even though they have lower gas sorption capacity because of low micropore volumes and surfaces (Ross and Bustin, 2009). Microporosity, which is positively correlated with TOC in shales (Chalmers and Bustin, 2007a,b), is a critical component of porous media owing to large internal surface areas and greater adsorption energies of <2 nm pores compared with that of larger pores of solids with similar compositions (Dubinin, 1975; Chalmers and Bustin, 2007a,b; Ross and Bustin, 2009). Thermally mature shales have larger micropore volume; therefore, the ratio of gas sorption capacity to TOC content is greater in thermally mature Devonian–Mississippian shales than in immature ones. Both TOC concentration and maceral composition are important when assessing methane adsorption capacity. Shales from the Lower Cretaceous Fort St. John Group of northeastern British Columbia have high methane capacities, corresponding to either high contents of inertodetrinite or vitrinite (Crosdale et al., 1998; Chalmers and Bustin, 2007a,b).

The increase in sorption capacity with increase in TOC and decrease in moisture content shows that the water molecule is sorbing to specific hydrophilic sites and that other available sorption sites are taken by the methane molecule. Consideration must also be given to the hydrophilic nature of clay minerals, which reduces gas adsorption capacity and the hydrophobic nature of organic matter, which provides available sites for gas adsorption in the presence of moisture (Ross and Bustin, 2009). Under moisture equilibrated conditions, moisture may render many microporous sorption sites unavailable to CH_4 by filling pore throats or occupying sorption sites (Joubert et al., 1974; Clarkson and Bustin, 1996, 1999, 2000; Bustin and Clarkson, 1998; Krooss et al., 2002; Busch et al., 2003; Ross and Bustin, 2007, 2008, 2009). Although the critical role of organic matter gas storage in shales is well documented and organic matter features (TOC content, type, thermal maturity), micropore structures and mineral compositions in shales greatly affect gas adsorption, details of the mechanism are not well understood. In particular, the effect of kerogen type and thermal maturity on gas sorption in shales is unclear and a quantitative model is not available to constrain these features under shale-gas reservoir pressure and temperature conditions.

In this study, a series of CH_4 adsorption isotherms on kerogens and organic rich shales were conducted at 35 °C, 50 °C and 65 °C at pressures up to 15 MPa. The main objectives of the study were to (1) explain the main control(s) on gas adsorption in organic rich shale gas systems; (2) quantitatively constrain the difference in organic matter type and thermal maturity on gas adsorption; (3) develop an empirical model of gas adsorption affected by organic matter features, temperature and pressure from experimental simulation; (4) predict adsorbed gas amount under geological shale-gas reservoir conditions; and (5) validate the developed model with previously published data. The quantitative model, which is based on the Langmuir equation parameters developed in this study, can be applied to specific organic matter properties. Our experimental findings have important implications for shale-gas resource assessments and recovery technologies.

2. Samples and experimental methods

2.1. Samples and sample preparation

Two sets of organic rich shale samples were used in this study. Geochemical characteristics of the samples are listed in Table 1.

The first set of samples collected from outcrops includes Green River Formation (Eocene, Utah), Woodford Shale (Upper Devonian, Oklahoma) and Cameo coal (Cretaceous, Colorado), which are representative of source rocks having typical type I, type II and type III kerogen, respectively. The calculated vitrinite reflectance values for these three samples, based on Rock–Eval pyrolysis T_{max} values, ranges from 0.55–0.58%, indicating low thermal maturity. Hydrogen indices for Green River, Woodford and Cameo samples are 872 mg/g TOC, 636 mg/g TOC and 239 mg/g TOC, respectively. For comparison purposes, kerogen concentrates of the bulk of Green River and Woodford samples were prepared by means of a conventional demineralization method by Humble Geochemical Services. Whole-rock samples and kerogen concentrates were used to investigate the effect of different organic matter types on gas adsorption.

A second set of samples was collected from Barnett Shale cores of different thermal maturity in three wells from the Fort Worth Basin, TX. The organic rich shale in a 1250 ft (380 m) section of the Lee C-5-1 well, Brown County, TX, contains 7.9% TOC and is considered a low maturity shale, with a calculated R_o of about 0.58%. The organic rich shale from the 6164 ft (1879 m) section of the Tarrant #A-3 well, Jack County, TX, is thermally mature, with a calculated R_o of around 0.81%. In contrast, the organic rich shale in the 7191 ft section (2192 m) of the Blakely well #1, Wise County, TX, is overmature, with a measured R_o of about 2.01%. This set of samples was used to investigate the effect of thermal maturity of organic matter on gas adsorption.

All samples were crushed using an 8000-ball mill/mixing machine and aliquots were ground to pass a sieve size of 500 μm (~100 mesh). The pulverized samples were dried in a 200 °C oven under a helium stream (2 ml/min) overnight for degassing and moisture removal. Around 4–6 g of rock sample, or about 1 g of kerogen or coal sample, was weighed using a 0.01 mg accuracy balance. Samples were then placed in stainless steel adsorption cells using a dry glass funnel. All adsorption measurements were performed on dry samples. Methane and helium gases of ultrahigh purity were provided by Airgas.

2.2. Experimental methods

2.2.1. CH_4 gas adsorption under high temperature and high pressure

2.2.1.1. Experimental setup. A scheme depicting the key elements of our volumetric adsorption apparatus is shown in Fig. 1. The experimental setup for pure gas adsorption basically consists of a reference volume for gas storage (volume V_r) and sample cell (volume V_s) connected by a 1/16″ tube. A set of manually actuated Valco and Swagelok valves and a high precision pressure transducer (max pressure 50 MPa, with a precision of 0.05%) are used to connect gas source supply, sample cell and reference cell and vacuum

Table 1
Geochemical characteristics of studied samples.

	Green River Fm. shale	Woodford Shale	Lee C-5-1 1250 ft	Tarrant A-3 6164 ft	Blakely #1 7191 ft	Cameo coal
TOC (%)	20.7	17.2	7.9	7.05	6.6	72.2
Kerogen type	Type I	Type II		Type II		Type III
S_1 (mg HC/g rock)	5.7	8.7	1.64	4.3	0.28	4.1
S_2 (mg HC/g rock)	180.2	109.2	43.5	14.7	1.07	175.3
S_3 (mg CO_2/g rock)	23.6	1.04	0.48	0.26	0.21	4.8
S_2/S_3	8	105	61	57	5	36
S_1/TOC (mg HC/g TOC))	26	51	37	61	4	6
T_{max} (°C)	440	430	430	443	561	429
R_o (%)	0.56_c	0.58_c	0.58_c	0.81_c	2.01_m	0.56_c
HI	872	636	551	209	16	239
OI	114	6	9	4	3	7
PI	0.03	0.07	0.06	0.23	0.21	0.02

Note: The 0.56_c value for R_o (%) is calculated from T_{max}, and 2.01_m is the measured value.

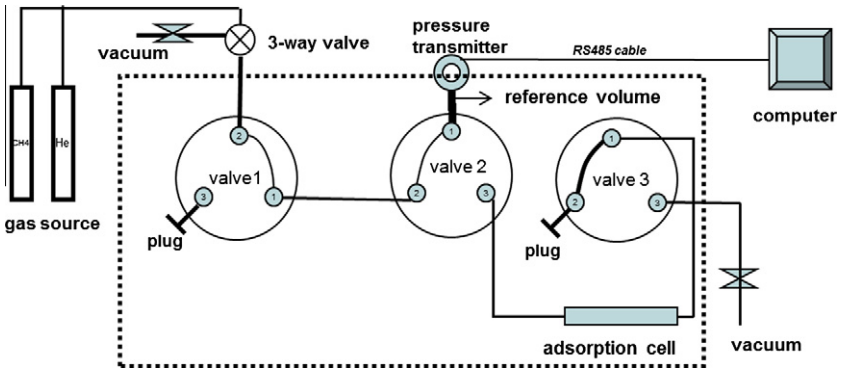

Fig. 1. Experimental set up for volumetric gas adsorption at high temperatures and pressures. GC oven thermostat outlined by dashed line.

pump. The reference cell volume is the volume between port 1 of valve 2 and the dead volume of the pressure transducer. Volumes of both reference cell and sample cell are determined by helium expansion in the presence and absence of a nickel cylinder of known density in a calibration procedure. The volumes of the reference volume and the sample cell are 2.38 ml and 7.15 ml, respectively, in the experimental setup. Reference volume, sample cell, pressure transducer (Series PA-33X/80801/5000PSIS, provided by Keller America) and Valco valves (VICI) are placed in an HP5890 GC oven (inner dashed line square in Fig. 1) and connected with 1/16″ tubes for gas supply and evacuation. A thermocouple was used for temperature measurement, with an accuracy within 0.1 °C. Variation of temperature and pressure was monitored and recorded by computer.

The pretreated rock or kerogen samples were placed into the sample cell. A 2 μm inline filter was used to prevent kerogen or mineral particles from entering the valves. A system leak test was performed after the loaded adsorption cell was connected to the experimental setup. The adsorption system, including both reference and adsorption cells, was first pressurized with helium gas to 15 MPa and the pressure change was then monitored for 2 h at a constant temperature (e.g., 35 °C). An acceptable leakage rate is 6.89×10^{-4} MPa/h.

2.2.1.2. Experimental procedure for adsorbed gas measurement. The experimental setup was evacuated with a vacuum pump (XDS10 Edwards) after the leak test was completed. The void volume in the adsorption chamber was measured with helium gas, which is considered an inert, non-sorbing gas (Lu et al., 1995; Krooss et al., 2002; Goodman et al., 2004; Keller and Staudt, 2005). Herein the void volume refers to the space that was not occupied by the solid sample in the adsorption cell. The amount of helium introduced from the reference cell to the adsorption cell was calculated on the basis of the pressure change in the reference volume before and after connecting it to the adsorption cell. Along with the incremental increase in pressure loading in the reference cell, gas charging to the adsorption cell was also achieved with a turn of the connecting valve 2. The void volume could be calculated on the basis of the following equation:

$$\frac{V_{void}}{V_r} = \frac{\rho_2 - \rho_3}{\rho_3 - \rho_1} \quad (1)$$

where V_{void} and V_r are the volume of the void volume of adsorption cell and the volume of the reference cell, respectively; gas density (ρ), in mol/cm^3, is calculated on the basis of the equations of state of McCarty and Arp (1990) and Setzmann et al. (1991). ρ_1 is helium gas density in the volume of ($V_{void} + V_r$) at pressure P_1 and a certain constant temperature (for example, 35 °C); ρ_2 is helium gas density in the reference cell (V_r) when pressure increases from P_1 to P_2 at the same temperature conditions; and ρ_3 is helium gas density in the volume of ($V_{void} + V_r$) when pressure decreases from P_2 to P_3 through gas expansion from the reference cell to the adsorption cell. Five void volume points were measured to ensure accuracy from a He pressure of 0.69 to 15 MPa. An average of these five measurements was taken as the void volume. Given the reasonable assumption that the void volume remains constant over temperatures ranging from 35–65 °C, one set of void volume measurements at 50 °C was applied to both 35 °C and 65 °C sample measurements in this study.

The CH_4 adsorption isotherm, which is the relation between amount of adsorbed CH_4 and gas pressure at a constant temperature, was measured after the leak test. The experimental setup was evacuated and then CH_4 was introduced into the reference cell. During isotherm measurement, a certain amount of CH_4 was

charged into the reference cell. After equilibrium was reached, as determined by monitoring the pressure until the variation was less than 6.9×10^{-4} MPa within a 5 min period, the valve between the reference cell and the sample cell was opened and the gas was expanded into the sample cell. By measuring the pressures before and after expansion, gas molar densities at different stages were calculated using an appropriate equation of state (EOS) and the amount of gas adsorbed at one pressure level could be determined. The isotherm was obtained by repeating these procedures until the measurement at the highest desired gas pressure was achieved. The amount of adsorbed gas (excess sorption), $N_{ads}(P)$ in mmol, at pressure, P, is given by (Lu et al., 1995):

$$N_{ads}(P) = N_{total}(P) - N_{ref}(P) - N_{void}(P) \quad (2)$$

where $N_{total}(P)$ is the total amount of gas charged into the system via the reference cell over the course of the experiment up to pressure P, $N_{ref}(P)$ is the amount of gas remaining inside the reference cell in equilibrium and $N_{void}(P)$ is the amount of gas that can be accommodated in the previously determined void volume V_{void} of the sample cell. At the ith pressure level, Eq. (2) can be rewritten as (Lu et al., 1995):

$$N_{ads}(i) = V_{ref}\sum_{j=1}^{i}[\rho_c(j) - \rho_e(j)] - V_{void}\rho_e(i)\ i = 1, 2, \ldots, n \quad (3)$$

where ρ_c is gas density in reference cell before gas expansion to the sample cell and ρ_e is gas density in both reference cell and sample cell in equilibrium after the gas was expanded. The thermophysical properties database of the US National Institute of Standards and Technology (NIST) was used for calculating the density of helium and methane at any given experimental temperature and pressure conditions on the basis of the equations of state of McCarty and Arp (1990) and Setzmann et al. (1991).

2.2.2. Langmuir equation and theoretical fitting of experimental adsorption isotherm

Adsorption is the accumulation of molecules on the surface of a material (adsorbent). This process creates a film of the adsorbate on the adsorbent's surface and is a consequence of surface energy minimization (Gregg and Sing, 1982). The adsorption process is generally classified as *physisorption* (characteristic of weak van der Waals force) or *chemisorption* (characteristic of covalent bonding). Adsorption is usually described through isotherms—i. e., the amount of adsorbed gas on the adsorbent as a function of its pressure at constant temperature. The quantity adsorbed is nearly always normalized by the mass of the adsorbent to allow comparison of different materials. The Langmuir equation or Langmuir isotherm is a model that relates the coverage or adsorption of gas molecules on a solid surface to gas pressure at a fixed temperature.

The monolayer adsorption theory states that a sorbent offers many nearly energetically homogenous adsorption sites (Gregg and Sing, 1982; Keller and Staudt, 2005) and the ratio of the amount of adsorbed gas (Γ) at a given pressure (P) to the Langmuir maximum amount of adsorbed gas ($\Gamma_{\max}$) on the sorbent is equivalent to the filled surface size (θ). Assuming that gas absorption in organic rich shales follows the monolayer adsorbates theory, CH_4 adsorption observed in our experiments can be expressed by the following Langmuir equation:

$$\Gamma = \Gamma_{\max}\frac{K \times P}{1 + K \times P} \quad (4)$$

where P is the pressure in MPa and K is the Langmuir constant in 1/MPa. The Langmuir pressure constant (P_L, in MPa), which is the reciprocal of the Langmuir constant, represents the pressure at which the amount of sorbed gas equals one-half of the maximum gas adsorption capacity—an important parameter for evaluating the feasibility of gas desorption under reservoir pressures. A least squares method was applied to fit our experimentally measured CH_4 adsorption isotherms by the Langmuir equation for determining Langmuir constants at 35 °C, 50 °C and 65 °C and Langmuir maximum adsorbed CH_4 amount.

The temperature dependence of Langmuir coefficient has been described by Xia et al. (2006) and Xia and Tang (2012). The Langmuir coefficient (k_a/k_d, the ratio of adsorption rate k_a to desorption rate k_d) can be obtained with Eq. (4) using sorption isotherms. Thermodynamic parameters of adsorption/desorption determine the Langmuir coefficient K. Entropies of adsorption have not been as intensively investigated as heats of adsorption (Xia and Tang, 2012). Entropy can be derived along with the isosteric heat of adsorption with Eq. (5) from the Langmuir coefficient K at several different temperature points.

$$K = \exp\left(\frac{q}{RT} + \frac{\Delta s^0}{R}\right) \quad (5)$$

where $q = E_a - E_d$ is the isosteric heat of adsorption; and $\Delta s^0 = R \ln(A_a/A_d)$ is the standard entropy of adsorption.

3. Results

3.1. CH_4 adsorption on isolated kerogens at 35 °C, 50 °C and 65 °C

CH_4 adsorption isotherms were measured on the three kerogen samples at 35 °C, 50 °C and 65 °C under a CH_4 equilibrium pressure of up to 15 MPa. The CH_4 sorption capacity of the kerogens at 50 °C decreased in the order: Cameo coal (type III) > Woodford kerogen (type II) > Green River kerogen (type I) (Fig. 2; Tables 2 and 3). Differences in specific surface area and different types of organic matter can result in variation of CH_4 sorption capacity, which is clearly a function of temperature and pressure (Fig. 3a–c).

Measured CH_4 adsorption isotherms at different temperatures can be well fitted by the Langmuir function (Figs. 2 and 3). Table 4 summarizes the Langmuir parameters obtained from the least square fit of experimental CH_4 adsorption isotherms. The Langmuir maximum CH_4 adsorption capacities for Green River kerogen, Woodford kerogen and Cameo coal are 0.78 mmol/g, 1.02 mmol/g and 1.01 mmol/g, respectively (Table 4). The TOC content of the Green River and Woodford kerogen concentrates is about 69.6% and 63.9%, respectively. The Langmuir maximum CH_4 adsorption capacity normalized to TOC is 1.22 mmol/g TOC, 1.46 mmol/g TOC and 1.40 mmol/g TOC for Green River kerogen, Woodford ker-

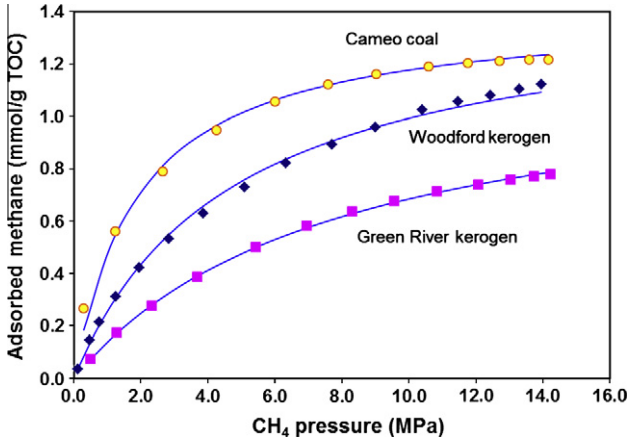

Fig. 2. Comparison of CH_4 sorption capacity for three different types of organic matter at 50 °C. Points are experimentally measured results and lines are Langmuir fitting results.

Table 2
Measured CH_4 sorption capacity for kerogens at different temperatures.

35.4 °C		50.4 °C		65.4 °C	
P (MPa)	CH_4 (mmol/g kerogen)	*P* (MPa)	CH_4 (mmol/g kerogen)	*P* (MPa)	CH_4 (mmol/g kerogen)
Green River Formation shale (type I) kerogen concentrates					
0.61	0.081	0.49	0.047	0.54	0.029
1.51	0.157	1.28	0.111	1.29	0.078
2.64	0.228	2.33	0.177	2.21	0.131
3.71	0.285	3.67	0.247	3.31	0.188
5.07	0.344	5.43	0.319	5.01	0.261
6.40	0.393	6.95	0.371	6.55	0.316
7.95	0.437	8.31	0.406	8.13	0.363
9.41	0.466	9.56	0.431	9.49	0.394
10.78	0.488	10.84	0.455	10.76	0.423
12.04	0.502	12.06	0.473	12.01	0.446
13.03	0.510	13.03	0.484	13.01	0.467
13.74	0.516	13.73	0.492	13.73	0.481
14.26	0.519	14.23	0.497	14.26	0.489
Woodford Shale (type II) kerogen concentrates					
0.14	0.050	0.11	0.023	0.79	0.084
0.38	0.140	0.48	0.101	1.54	0.161
0.85	0.232	0.76	0.148	2.63	0.259
1.41	0.304	1.26	0.216	3.87	0.339
2.15	0.387	1.94	0.293	5.29	0.416
3.16	0.469	2.83	0.369	6.77	0.463
4.23	0.537	3.86	0.439	8.39	0.525
5.51	0.600	5.09	0.508	9.95	0.563
6.79	0.651	6.33	0.571	11.34	0.607
8.16	0.692	7.71	0.621	12.54	0.636
9.83	0.733	9.01	0.667	13.42	0.651
11.24	0.768	10.41	0.713	14.06	0.667
12.41	0.783	11.47	0.734		
13.27	0.793	12.43	0.752		
13.91	0.795	13.31	0.768		
		13.95	0.781		
Cameo coal (type III)					
0.38	0.288	0.29	0.193	0.63	0.171
1.32	0.505	1.24	0.405	1.69	0.358
2.42	0.645	2.65	0.571	3.00	0.499
3.58	0.740	4.26	0.684	4.46	0.598
5.13	0.822	6.00	0.762	6.02	0.669
6.58	0.872	7.59	0.810	7.56	0.719
7.88	0.905	9.03	0.839	9.13	0.757
9.30	0.926	10.60	0.860	10.58	0.784
10.57	0.937	11.76	0.869	11.92	0.805
11.78	0.942	12.70	0.873	13.02	0.819
12.97	0.943	13.58	0.877	13.79	0.828
13.77	0.942	14.17	0.879		

Note: Unit conversion factor: 1 mmol/g = 711.42 scf./ton.

ogen and Cameo coal, respectively. In contrast, the Langmuir constant increases with kerogen type in the following sequence: type I < type II < type III (Table 4).

3.2. CH_4 adsorption on bulk rocks at 35 °C, 50 °C and 65 °C

For comparison purposes, CH_4 adsorption isotherms for the Green River Formation and Woodford Shale bulk rock samples were each measured at 35 °C, 50 °C and 65 °C. Comparisons of CH_4 adsorption isotherms for shale samples and isolated kerogen samples are shown in Fig. 4. The amount of CH_4 adsorbed per gram TOC is clearly larger for the isolated kerogens than for the bulk shales. The lower level of gas adsorption in the whole rocks may indicate that the presence of inorganic minerals in the rock matrix shields active sorption sites on the organic matter. The observed trend for CH_4 adsorption capacity as a function of temperature and the equilibrium pressure in the whole rock samples is similar to that of the isolated kerogen samples (Fig. 5; Table 3).

The experimental CH_4 adsorption isotherms on bulk shales at different temperatures were also fitted using the Langmuir adsorption model. There is fairly good agreement between calculated and experimentally observed isotherms (Fig. 5; Table 3). Langmuir maximum CH_4 adsorption capacities for Green River and Woodford shales are 0.23 mmol/g rock and 0.21 mmol/g rock (Table 4), respectively. The Langmuir maximum CH_4 adsorption capacity normalized to TOC is 1.13 mmol/g TOC and 1.21 mmol/g TOC for shales of the Green River and Woodford, respectively.

3.3. CH_4 adsorption on organic rich shales of different thermal maturities at 35 °C, 50 °C and 65 °C

The effect of thermal maturity on CH_4 adsorption was determined for three Barnett Shale samples with measured vitrinite reflectance values of 0.58, 0.81 and 2.1 %R_o and TOC contents ranging from 6.6–7.9%. CH_4 adsorption isotherms for these samples were measured at 35 °C, 50 °C and 65 °C at CH_4 equilibrium pressures of as high as 15 MPa. A comparison of the 50 °C CH_4 sorption isotherms for these samples is shown in Fig. 6. The measured CH_4 adsorption isotherms were fitted by the Langmuir function with good results (Figs. 5 and 6). The maximum Langmuir CH_4 absorption capacity for Lee C-5-1 (R_o = 0.58%), Oxy Tarrant #3 (R_o = 0.81%) and Blakely #1 is 0.15 mmol/g, 0.14 mmol/g and

Table 3
Measured CH_4 sorption capacity for organic-rich shales at differenet temperature.

35.4 °C		50.4 °C		65.4 °C	
P (MPa)	CH_4 (mmol/g rock)	*P* (MPa)	CH_4 (mmol/g rock)	*P* (MPa)	CH_4 (mmol/g rock)
Green River Formation shale (TOC = 20.7%, R_o = 0.55%)					
0.92	0.034	0.74	0.016	0.86	0.015
2.19	0.062	1.75	0.034	2.01	0.035
3.81	0.089	3.01	0.053	3.35	0.053
5.41	0.109	4.52	0.072	4.98	0.072
6.93	0.123	6.22	0.092	6.59	0.088
8.57	0.135	8.09	0.107	8.17	0.101
9.97	0.144	9.86	0.120	9.93	0.114
11.46	0.150	11.51	0.129	11.53	0.123
12.66	0.154	12.84	0.135	12.67	0.129
13.43	0.156	13.73	0.139	13.42	0.132
13.92	0.157	14.32	0.142	13.91	0.135
Woodford Shale (TOC = 17.2%, R_o = 0.58%)					
0.21	0.014	0.15	0.008	0.13	0.004
0.86	0.038	0.64	0.023	0.52	0.013
1.82	0.061	1.43	0.043	1.22	0.028
3.04	0.082	2.52	0.063	2.09	0.043
4.42	0.101	3.78	0.082	3.11	0.059
6.26	0.121	5.23	0.100	4.43	0.075
8.04	0.134	6.57	0.112	5.89	0.090
9.72	0.142	8.07	0.123	7.15	0.101
11.02	0.147	9.52	0.131	8.30	0.110
12.12	0.149	10.70	0.137	9.39	0.117
13.20	0.151	11.93	0.142	10.34	0.123
14.01	0.153	13.16	0.145	11.30	0.128
		13.98	0.148	12.21	0.132
				13.06	0.136
				13.93	0.139
Barnett Shale (Lee C-5-1, 1250 ft, TOC = 7.9%, R_o = 0.58%)					
0.84	0.026	0.70	0.017		
1.69	0.044	1.61	0.036		
2.53	0.058	2.56	0.052		
3.31	0.069	3.49	0.064		
4.16	0.078	4.43	0.075		
5.02	0.086	5.33	0.085		
5.93	0.093	6.31	0.092		
6.74	0.097	7.24	0.099		
7.52	0.102	8.24	0.104		
8.34	0.105	9.20	0.108		
9.19	0.107	10.12	0.109		
10.10	0.109	11.08	0.111		
11.04	0.109	12.05	0.114		
		13.09	0.114		
		13.80	0.115		
Barnett Shale (Tarrant A-3, TOC = 7.05%, R_o = 0.81%)					
0.44	0.016	0.46	0.013	0.28	0.004
1.19	0.032	0.96	0.023	1.06	0.019
2.11	0.047	1.42	0.032	2.10	0.033
3.19	0.060	1.99	0.040	3.36	0.047
5.00	0.075	2.76	0.050	4.74	0.060
6.79	0.085	3.59	0.059	6.12	0.073
8.43	0.095	4.65	0.068	7.73	0.083
9.98	0.101	5.90	0.077	9.22	0.090
11.48	0.103	7.19	0.084	10.64	0.095
12.89	0.103	8.51	0.090	11.93	0.099
13.81	0.103	9.77	0.094	13.12	0.102
14.43	0.103	11.09	0.099	13.92	0.105
		12.35	0.100		
		13.18	0.102		
		14.02	0.104		
Barnett Shale (Blakely #1, 7191 ft, TOC = 6.6%, R_o = 2.01%)					
0.04	0.011	0.20	0.014	0.11	0.007
0.31	0.024	0.55	0.026	0.35	0.015
0.62	0.036	1.04	0.038	0.65	0.023
1.01	0.046	1.56	0.048	0.99	0.031
1.53	0.057	2.04	0.056	1.46	0.039
2.21	0.068	2.80	0.065	2.13	0.049
3.17	0.079	3.96	0.076	3.10	0.060
4.79	0.092	5.44	0.086	4.28	0.070
6.34	0.100	6.99	0.093	5.70	0.080
7.79	0.104	9.21	0.097	7.47	0.089

(*continued on next page*)

Table 3 (*continued*)

35.4 °C		50.4 °C		65.4 °C	
P (MPa)	CH_4 (mmol/g rock)	*P* (MPa)	CH_4 (mmol/g rock)	*P* (MPa)	CH_4 (mmol/g rock)
9.22	0.107	11.08	0.099	9.20	0.094
10.57	0.108	12.72	0.100	11.15	0.098
11.94	0.107	13.83	0.100	12.82	0.100
13.23	0.106			13.91	0.101
14.09	0.105				

Note: Unit conversion factor: 1 mmol/g = 711.24 scf/ton.

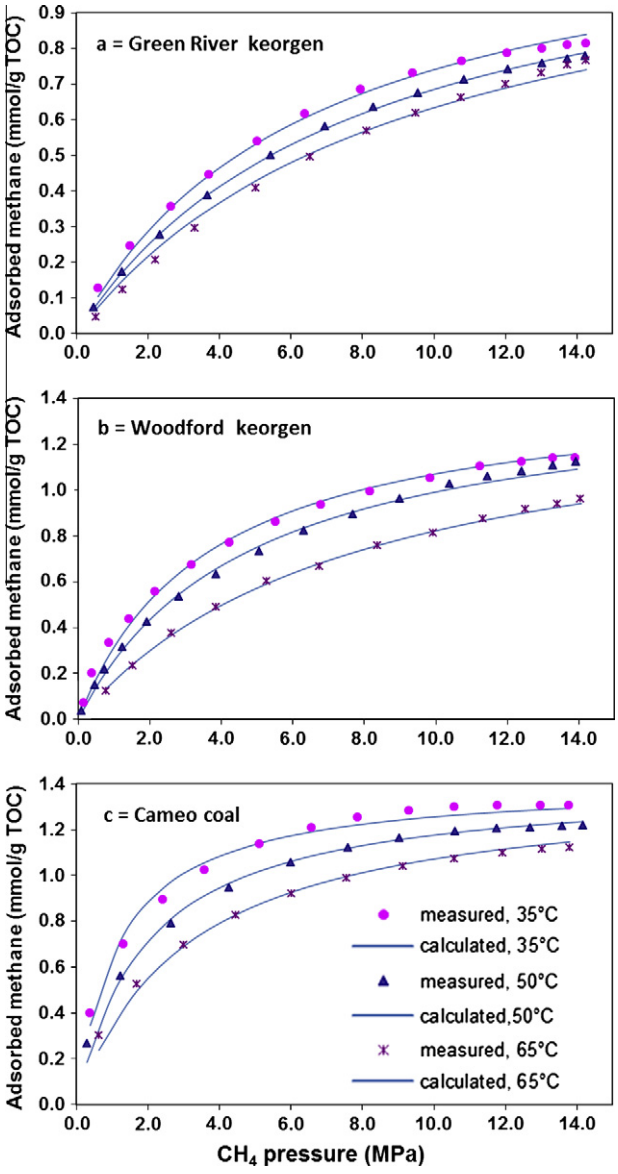

Fig. 3. CH_4 adsorption isotherms for kerogen at three different temperatures. a = Green River kerogen (type I), b = Woodford kerogen (type II) and c = Cameo coal (type III). Points are experimentally measured results and lines are Langmuir fitting results.

0.12 mmol/g rock, respectively (Table 4). Differences among the samples can largely be attributed to differences in organic matter content. When normalized to TOC, maximum Langmuir CH_4 absorption capacities are 1.96 mmol/g TOC, 2.03 mmol/g TOC and 1.83 mmol/g TOC, respectively. Adsorption capacity is just slightly lower for high maturity organic matter than that for lower maturity.

Langmuir constants are greater for high maturity samples than for low maturity samples (Table 4). In consequence, the "Langmuir pressures, P_L [MPa]", defined as the reciprocal of Langmuir constants are highest for the low maturity samples. For example, at 50 °C, the Langmuir constants for the Lee C-5-1 and Oxy Tarrant #A-3 samples (R_o = 0.56%) are in the range of 0.194–0.195/MPa (corresponding to Langmuir pressures of 5.15–5.12 MPa), while a much higher Langmuir constant (0.428/MPa) and, correspondingly a lower Langmuir pressure (P_L = 2.33 MPa) was found for the more mature Blakely #1 sample (R_o = 2.01%). This indicates that CH_4 is adsorbing more readily at lower pressures on higher maturity kerogens. This also implies that, due to this higher affinity, the adsorbed methane is released less readily from highly mature kerogen and the partial pressure has to be reduced more strongly to desorb the gas.

4. Discussion

4.1. Effect of organic matter type on gas adsorption

The Langmuir constant is related to the affinity of a gas for a surface (i.e., larger values indicate stronger affinity of the gas for the sorbent). For the samples examined in this study, the value of the Langmuir constant varies directly with kerogen type: type I kerogens exhibit the lowest Langmuir constants and type III kerogens exhibit the highest (Fig. 7a). These results indicate that differences in the chemical structure of organic matter play an important role in CH_4 adsorption in organic rich rocks. The progression from type I to type III kerogen involves a consistent shift toward lower H/C ratios, as is reflected in the HI values determined from Rock–Eval pyrolysis (Table 1). This progression is accompanied by a relative increase in the proportion of aromatic hydrocarbons relative to the aliphatic and naphthenic hydrocarbons (Tissot and Welte, 1984; Helgeson et al., 2009). Our results show that aromatic rich kerogens may have a stronger affinity for methane than kerogens containing more aliphatic organic matter. The details of the mechanism for this are not well understood and this is an area that merits further investigation.

The effect of the difference in organic matter type on Langmuir constant can be quantified with sorption isotherms. A least squares fit was applied to our experimentally measured CH_4 adsorption isotherms based on the Langmuir function for determining Langmuir constants at 35 °C, 50 °C and 65 °C, as well as Langmuir maximum adsorption capacity. A clear linear relation exists between the natural logarithm of the Langmuir constant (K) and the reciprocal of temperature ($1/T$) (Fig. 7). A linear relation between the Langmuir constant and a reciprocal of temperature is defined by our experiments on the impact of organic matter type on gas adsorption. Empirical Eqs. (6)–(8) were derived from this study:

$$\ln(K) = 1241/T - 5.89 \quad \text{for type I kerogen} \tag{6}$$

$$\ln(K) = 2628/T - 9.75 \quad \text{for type II kerogen} \tag{7}$$

$$\ln(K) = 3366/T - 11.06 \quad \text{for type III kerogen} \tag{8}$$

Table 4
Langmuir fitting results for methane adsorption for the bulk of shales and isolated kerogen samples.

		Woodford Shale		Green River Fm. shale		Lee C-5-1	Oxy Tarrant #A-3	Blakely #1	Cameo coal
		Rock	Kerogen	Rock	Kerogen	Rock	Rock	Rock	Rock
TOC (%)		17.2	69.6	20.7	63.9	7.9	7.1	6.6	72.2
R_o (%)		0.58_c		0.56_c		0.58_c	0.81_c	2.01_m	0.56_c
Langmuir maximum (mmol/g rock)		0.21	1.02	0.24	0.78	0.16	0.14	0.12	1.01
Langmuir maximum (mmol/gTOC)		1.21	1.46	1.14	1.22	1.96	2.03	1.83	1.40
Langmuir constant (1/MPa)	35.4 °C	0.22	0.28	0.16	0.15	0.25	0.22	0.64	0.85
	50.4 °C	0.18	0.21	0.10	0.13	0.19	0.20	0.43	0.52
	65.4 °C	0.14	0.13	0.09	0.11		0.17	0.34	0.32

Note: Unit conversion factor: 1 mmol/g = 711.24 scf./ton.

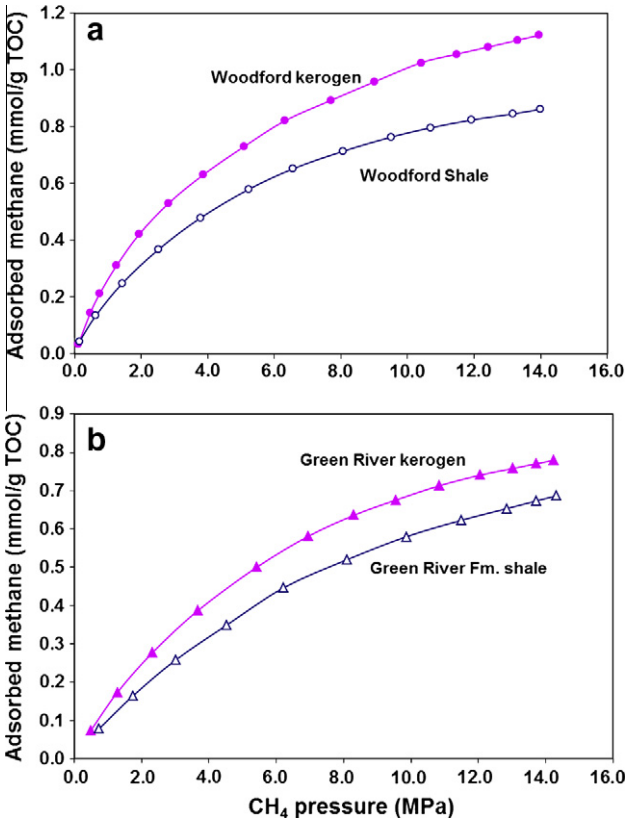

Fig. 4. Comparison of CH_4 sorption capacity on bulk-rock samples (Green River Formation and Woodford Shale) and their kerogen separates at 50 °C.

where T is temperature in degrees Kelvin and K is the Langmuir constant in units of 1/MPa. Note that the above, empirical linear regressions were obtained from low maturity kerogen. Differences in kerogen thermal maturity, the presence of clay minerals and moisture content may alter this relation (Joubert et al., 1974; Clarkson and Bustin, 1996, 1999, 2000; Bustin and Clarkson, 1998; Krooss et al., 2002; Busch et al., 2003; Ross and Bustin, 2007, 2008, 2009; Fathi and Akkutlu, 2009). In this study, we did not quantitatively investigate the effect of mineral components on gas adsorption. However, gas adsorption isotherms on isolated kerogen and the corresponding bulk rocks of Green River and Woodford shales were compared to evaluate the possible effects of the mineral matrix in Eqs. (6) and (7). Langmuir constants at different temperatures for the bulk rock samples of Green River and Woodford shales fall on or near the lines defined by their kerogen concentrates (Fig. 7a), suggesting that gas adsorption is controlled mainly by organic matter and that minerals play a relatively insignificant role in gas adsorption within organic rich shales.

For thermally immature organic rich rocks, the relation between organic matter type and methane adsorption capacity (as defined by the Langmuir maximum) is complex. When normalized to the TOC content, the type I kerogen in whole rock samples from the Green River Formation has the lowest CH_4 sorption capacity (1.14 mmol/g TOC). This is followed by the type II kerogen in the whole rock sample of the Woodford Shale (1.21 mmol/g TOC) and then the type III kerogen of the Cameo coal (1.40 mmol/g TOC). However, the immature Barnett Shale (type II kerogen) sample from the Lee C 5-1 well has the highest gas sorption capacity of any immature sample examined with 1.96 mmol CH_4/g TOC. The widely used type I, II and II classification scheme for kerogen is not adequate to fully understand the relation between organic matter type and gas sorption capacity in organic rich rocks and a more detailed examination of the nature of the organic matter will be required. Previous studies on coals have indicated that maceral composition influences the gas sorption capacity and the pore structure of the macerals has been suggested as a possible explanation for this relation (Clarkson and Bustin, 1996; Krooss et al., 2002; Li et al., 2010). Other researchers have reported an increase in gas sorption capacity with increasing vitrinite content, suggesting a prominent role of this maceral in gas adsorption in coals (e.g. Lamberson and Bustin, 1993; Levine et al., 1993). This approach could be applied to organic rich shales to further our understanding of the relation between organic matter type and gas sorption capacity.

4.2. Effect of the thermal maturation of organic matter on gas adsorption

With increasing thermal maturation, the hydrogen index of organic matter in shales decreases as a result of kerogen conversion to hydrocarbons (Behar and Vandenbroucke, 1987; Behar et al., 1992). This is due to the fact that at high thermal maturation levels, the remaining organic matter is intensively aromatized (Tissot and Welte, 1984). Our results indicate that organic matter thermal maturation can significantly affect gas adsorption in shales. In particular, at 50 °C, the Langmuir constants (K) for the three Barnett Shale samples of different maturities (Blakely #1, Tarrant #3-A shale and Lee C-5-1) are 0.428, 0.195 and 0.194/MPa, respectively (Fig. 7b and Table 4). At lower pressures, CH_4 sorption capacity on the Blakely #1 shale is larger than that on both the Lee C-5-1 and Tarrant #A-3 shales which have low to medium thermal maturity. When superimposing the correlation of the ln(K) and the reciprocal of adsorption temperature for typical type I, II and III kerogen (Green River Formation, Woodford Shale and Cameo coal, respectively) defined by Eqs. (6)–(8), we observed that Langmuir constants of low and medium maturity Barnett Shale samples are in the line with the type II kerogen trend (Fig. 7b). In contrast, the Langmuir constant for the Blakely sample with high thermal maturity ranges around the type III kerogen trend line (Fig. 7b). The application of Eqs. (6) and (7) can be further constrained by consid-

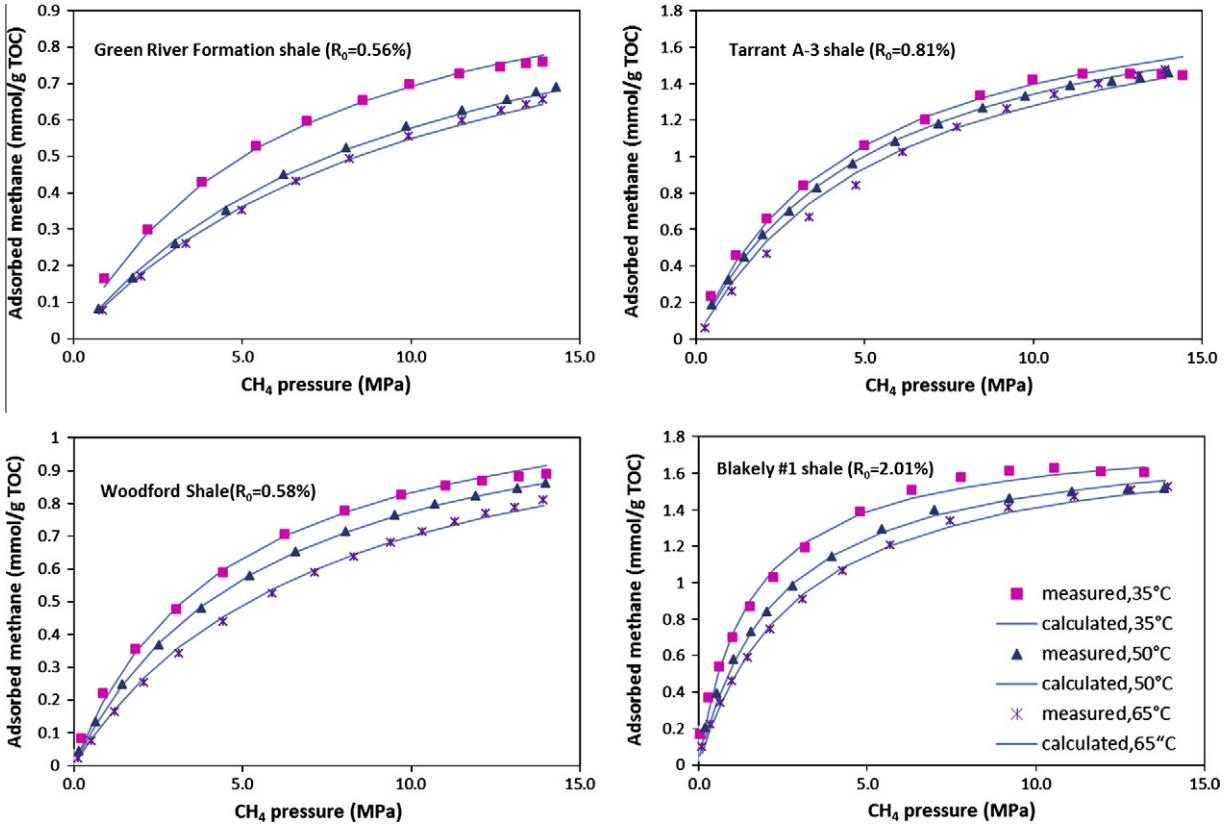

Fig. 5. CH_4 adsorption isotherms for shales at three different temperatures. Points are experimentally measured results and lines are Langmuir fitting results.

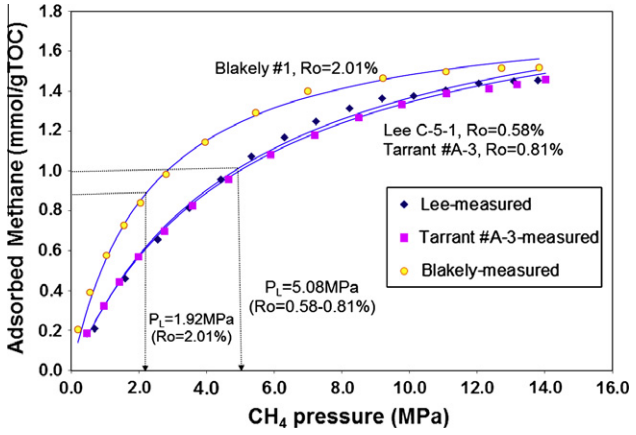

Fig. 6. Comparison of CH_4 sorption capacity on Barnett Shale samples of various thermal maturities at 50 °C.

ering the differences in both organic matter types and thermal maturity. Eqs. (9) and (10) include the effect of organic matter thermal maturation on gas adsorption:

$$\ln(K) = 2628/T - 9.75 \quad \text{for type II kerogen with } R_o < 1.4\% \quad (9)$$

$$\ln(K) = 3366/T - 11.06 \quad \text{for type II kerogen with } R_o > 1.4\% \quad (10)$$

where T is temperature in degrees Kelvin and K is the Langmuir constant with a unit of 1/MPa. Given the still relatively small data base, these correlations are rather preliminary. On the other hand, maturation of all kerogen types will invariably lead to a higher degree of aromatization, which is a characteristic feature of type III kerogen from the very beginning.

4.3. Effect of organic matter on thermodynamic parameters for adsorption

The isosteric heat of adsorption (q) and the standard entropy of adsorption (Δs^0) are two important thermodynamic parameters which can be used for describing the temperature dependence of the Langmuir constant at a given temperature. Both of these parameters for organic rich shales and kerogen concentrates were calculated according to Eq. (5) and are listed in Table 5. The heats of adsorption determined for type I, II and III kerogen are 10.3, 21.9 and 28 kJ/mol, respectively, and these values are similar to the previously reported quantities for coal (Table 5). The observed trend of increasing heat of adsorption for type I to type III kerogens is consistent with the Langmuir constants for these samples. The differences in the heats of adsorption determined for different kerogens are likely related to differences in the chemical structures present in the kerogens. As discussed above, compared to type I and II kerogens, type III kerogen contains relatively more aromatic moieties that may enhance CH_4 adsorption.

The entropy of adsorption reflects the restricted mobility of adsorbed molecules (Xia et al., 2006). The entropy of physisorption should be close to the loss of translational entropy from three dimensional free gas to two dimensional adsorbates and this entropy loss is −82 to −87 J/mol/K at temperatures of 273–423 K for methane molecules (Xia and Tang, 2012). While Δs^0 for methane adsorption on the whole rock shale samples studied is close to this value (−54.2 to −64.5 J/mol/K), the values for Woodford kerogen and Cameo coal are much more negative and the values for Green River kerogen and Tarrant #A-3 rock are much less negative (Table 5). The excessively negative values observed for the Woodford kerogen and Cameo coal samples may indicate that in addition to the predominant physisorption processes there is some slight amount of chemical interaction, or chemisorption, between CH_4

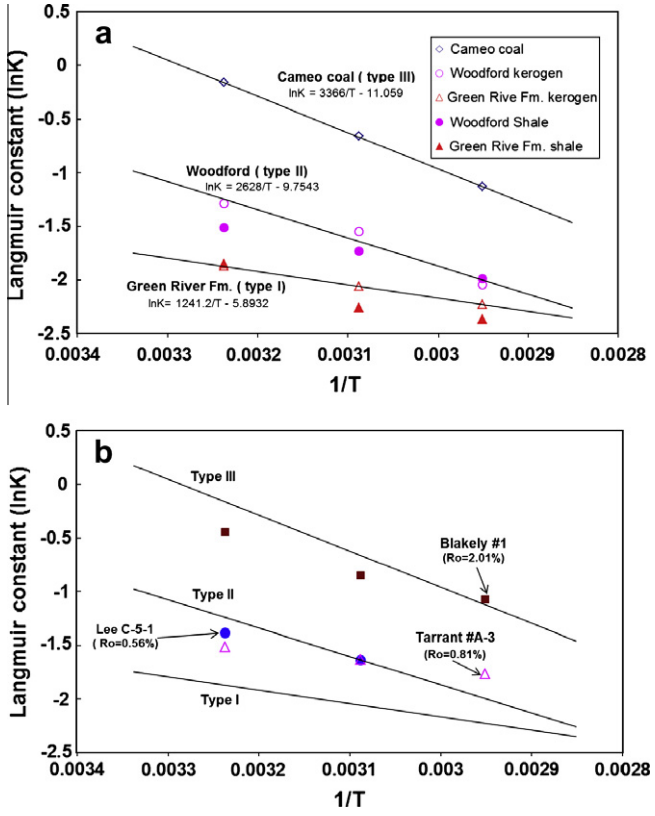

Fig. 7. Plots showing the temperature dependence of the Langmuir constant (K) for organic matter (a) and thermal maturity (b). Regression lines obtained for organic matter (a) are plotted for comparison in (b). Note that Langmuir constant varies directly with both kerogen type (a) and increasing maturity (b).

Table 5
Thermodynamic parameters of CH_4 adsorption on different materials.

Adsorbent	q (kJ mol^{-1})	Δs (J mol^{-1} K^{-1})
Green River kerogen (type I)	10.3	−49.0
Woodford kerogen (type II)	21.9	−81.1
Cameo coal (type III kerogen)	28.0	−92.2
Green River rock	15.1	−64.5
Woodford rock	15.3	−57.2
Lee C-5-1 rock	14.0	−56.9
Oxy Tarrant #A-3 rock	7.3	−36.2
Blakely #1 rock	18.4	−63.4
Coal	10–22[a], 15.1[b]	−76.0[b]
Activated carbon	16–20[c]	−62.8[d]
Zeolite	15.7[e]	−55.9[f]

[d] Calculated from Himeno et al. by Xia and Tang (2012).
[e] Cavenati et al. (2004).
[f] Calculated from Cavenati et al. (2004).
[a] Ruppel et al. (1974).
[b] Calculated from Clarkson et al. (1997) by Xia and Tang (2012).
[c] Düren et al. (2004), Himeno et al. (2005).

and the kerogen in these samples. Because the Barnett Shale sample (Tarrant #A-3) is in the oil window (%R_o = 0.81) it is possible that heavier hydrocarbon molecules (i.e., oil) are present on adsorbent surfaces in the kerogen and that some or all of the CH_4 may be dissolved in, or adsorbed onto the surface of, this oil rather than adsorbed on kerogen. This could account for the higher entropy determined for the Tarrant #A-3 sample. However, this explanation cannot be applied to the Green River kerogen sample because it has a much lower thermal maturity (%R_o = 0.56) and the kerogen isolation procedure involves solvent extraction which removes soluble hydrocarbons. Further research is needed to understand the anomalously high entropy value determined for the Green River Formation kerogen. The above correlations from which these entropies are derived are based on limited (three) data points and more detailed information is needed to determine the accuracy and reproducibility of the thermodynamic parameters based on sorption measurements.

The thermodynamic parameters derived for the maturity suite in the Barnett Shale do not show a consistent trend. While the lowest maturity sample (Lee C 5-1) has a lower heat of absorption and less negative entropy value than the highest maturity sample (Blakely #1), the intermediate maturity sample (Oxy Tarrant #A-3) actually has the smallest heat of adsorption and the least negative entropy value. As discussed above, this is probably the result of the Oxy Tarrant #A-3 being in the oil window (%R_o = 0.81). The low maturity (%R_o = 0.58) Lee C 5-1 sample has not generated significant amount of liquid hydrocarbons and the high maturity (%R_o = 2.01) Blakely #1 sample has certainly generated and expelled all of the liquid hydrocarbons that can be produced. The problems related to the presence of liquid hydrocarbons notwithstanding, these results indicate that the affinity of CH_4 molecules for organic matter increases with increasing thermal maturity in organic rich rocks.

4.4. Gas adsorption capacity and organic matter content (TOC)

Maximum Langmuir CH_4 adsorption capacity in organic rich shales is greatly affected by TOC content. As shown in Fig. 8, Langmuir CH_4 adsorption capacity increases linearly with increasing TOC concentration. Eq. (11) gives a linear regression between Γ_{max} and TOC content that is based on our experimental measurements. The regression provides an empirical basis on which to estimate the Langmuir maximum CH_4 adsorption capacity as TOC is measured in a shale-gas reservoir.

$$\Gamma_{max} = 1.34 \times \mathrm{TOC} + 0.0148 \quad (11)$$

where Γ_{max} is in mmol (CH_4)/g rock and TOC is the total organic carbon content in wt%. The correlation was obtained from sorption isotherms in the temperature up to 65 °C.

A similar correlation between gas sorption capacity and TOC content at 30 °C and 6 MPa pressure has been observed in previous studies (Chalmers and Bustin, 2007a,b; Ross and Bustin, 2007, 2009). Variations in organic matter types and thermal maturity can result in variations in pore structure and pore size within organic matter (Ross and Bustin, 2007, 2009; Loucks et al., 2009). These variations can greatly affect the availability of surface area for methane adsorption. For example, pore characterization of siliceous mudstones from the Mississippian Barnett Shale of the Fort

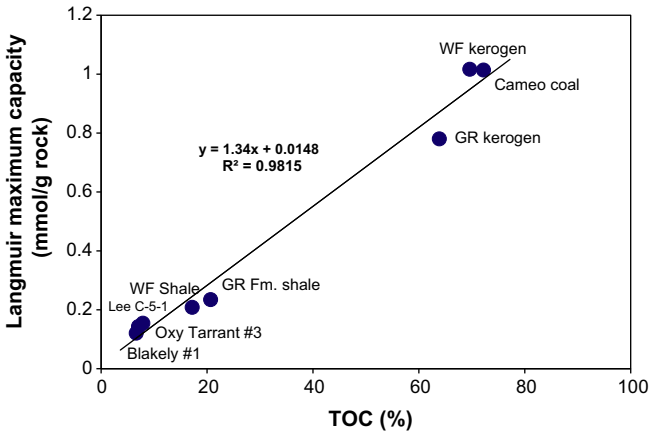

Fig. 8. Linear relation between Langmuir maximum capacity and TOC in shales.

Worth Basin, Texas, shows that these rocks dominantly contain 5–750 nm nanopores that occur mostly in organic matter grains as intraparticle pores (Loucks et al., 2009). The abundance of pores in organic matter is related directly to thermal maturity, with pores being observed only in organic matter at thermal maturities greater than about 0.60 $\%R_o$. Most of these nanopores are formed during thermal decomposition of organic matter during hydrocarbon generation (Loucks et al., 2009). Behar and Vandenbroucke (1987) reported that pores of 5–50 nm size developed in high maturity kerogen, the size of pores depending on the type of kerogen hosting the pores.

Gas sorption capacity in organic rich shales is greatly reduced in the presence of moisture (Ross and Bustin, 2009). Moisture content is thus an important factor in gas-shale reservoir systems because the amount and distribution of water can limit the volume of sorbed and free gas and relative permeability/diffusivity. Variations in moisture content depend on mineralogy, maturity, kerogen type and pore size distribution. Measurements of gas sorption capacity of Devonian–Mississippian shales in the WCSB under dry and moisture equilibrated conditions (Ross and Bustin, 2009) showed that sorption capacity under dry conditions is substantially greater than under moisture equilibrated conditions (Fig. 9). This observation suggests that, when present, moisture partly occupies available surface sites of organic rich shales, resulting in low sorption capacity for methane.

Our empirical relationships between sorption capacity and organic matter type and thermal maturity can be used to elucidate the effect of moisture content on gas adsorption capacity in shale-gas systems. The empirical relation of Eq. (11) is used to determine Langmuir maximum gas adsorption capacity at a given TOC content and the empirical relations of Eqs. (9) and (10) are used to determine the Langmuir constant at 30 °C for type II organic matter with different thermal maturities. After Langmuir maximum gas adsorption capacities for shales of various TOC and Langmuir constants at a given temperature are determined, gas sorption capacity at 30 °C and 6 MPa can be calculated for shales of differing TOC contents according to the empirical relation of Eq. (4). A good agreement of our model (blue lines, Fig. 9) with the moisture equilibrated gas sorption capacity values reported by Ross and Bustin (2009) was obtained. The two solid lines in Fig. 9 are for type II organic matter of different maturities, the upper line is for $R_o > 1.5\%$ and the lower line is for $R_o < 1.2\%$. The result supports the notion that TOC content is the primary control on CH_4 sorption in these shale systems.

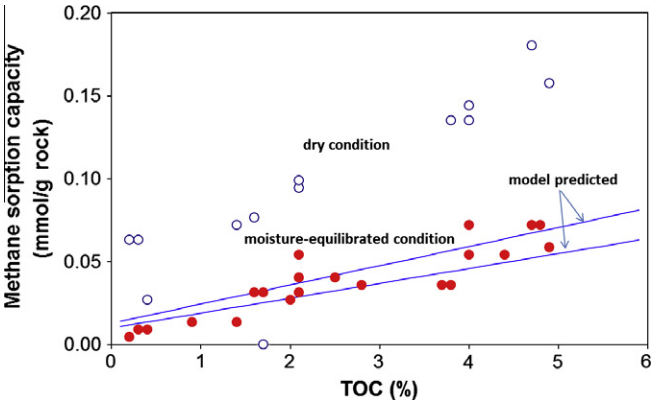

Fig. 9. Methane sorption capacity of dry and moisture equilibrated shales samples at 30 °C and 6 MPa as a function of TOC content. Red filled circles and blue open circles denote samples measured by Ross and Bustin (2009) at 30 °C and 6 MPa under moisture equilibrated and dry conditions, respectively. (For interpretation of the references to colour in this figure legend, the reader is referred to the web version of this article.)

Note that our model shows a good agreement with the measured CH_4 sorption capacity under moisture equilibrated conditions. Our model focuses on the effect of organic matter on gas sorption and has been derived under dry conditions. Our hypothesis is that moisture mainly occupies the surface sites of hydrophilic clay minerals but does not cover the surface of organic matter, which behaves hydrophobically. Therefore, the distribution of hydrophobic and hydrophilic sorption sites throughout the network of shale-gas reservoirs would play a major role in the selective sorption of CH_4 and moisture, which could be indicated by gas sorption capacities with different moisture contents. The offset of about 0.07 mmol/g rock between measured CH_4 sorption capacity at dry versus moisture equilibrated conditions might result from a large exposure of the surface area of clays and then significant increase of gas sorption capacity under dry conditions. This issue needs to be addressed further in future research.

5. Conclusions

Our studies of CH_4 sorption characteristics of bulk samples of organic rich shales and kerogen isolated from such shales reveal important cause and effect relations between organic matter type and thermal maturity and gas adsorption. Significant conclusions are as follows: Organic matter is a primary control on gas adsorption in shale-gas systems: generally, the higher the TOC content, the greater the gas-sorption capacity. Differences in organic matter type greatly affect gas sorption rates in organic rich shales. The value of the Langmuir constant varies directly with kerogen type: type I < type II < type III. There is a small but significant difference in Langmuir maximum sorption capacity, with type I kerogen being lower than types II or III and this relation is possibly a product of increasing kerogen aromaticity. Organic matter thermal maturation mainly affects the gas sorption capacity on organic rich shales at lower pressure; gas sorption capacity is higher in shales with higher thermal maturity. The Langmuir pressure for the highest maturity Barnett Shale samples ($\% R_o > 2.01$) is about half that of the low maturity samples ($\%R_o = 0.56$) under the same temperature conditions. The presence of moisture can greatly reduce gas sorption capacity. Our hypothesis is that moisture mainly occupies surface sites of hydrophilic clay minerals, causing these particles to swell and block pore throats, which would reduce porosity–permeability and restrict access to active sites. This is an issue that needs to be addressed quantitatively in future research.

Acknowledgments

This research is a part of research results of the EM/BEG unconventional reservoir project, which is financially supported by ExxonMobil, 2012CB214701, 20100559 and the Jackson School of Geosciences, The University of Texas at Austin. The construction of an in-house high temperature and pressure gas adsorption system was funded by the Jackson School of Geosciences start-up funds. The Bureau's Mudrock Systems Research Laboratory consortium and State of Texas Advanced Resource Recovery program (STARR program) provided funding and access to Barnett Shale cores and TOC and Rock-Eval data. Thanks to Dr. Mike Lewan for providing the Green River Formation sample. Drs. Bob Dias, Dick Keefer in USGS Denver reviewed our manuscript and provided suggestions to greatly improve the quality of the manuscript. In particular, we would like to thank Drs. Xinyu Xia, Bernhard Krooss and Yongchun Tang as reviewers who provided constructive suggestions that significantly improved the quality of the manuscript. Publication authorized by the Director, Bureau of Economic Geology. Any use of trade, product or firm names is for descriptive pur-

poses only and does not imply endorsement by the US Government.

Associate Editor—**Maowen Li**

References

Ambrose, R.J., Hartman, R.C., Campos, M.D., Akkutlu, I.Y., 2011. Multi-component Sorbed Phase Considerations for Shale Gas-in-place Calculations. Society of Petroleum Engineers, Paper SPE-141416, 10p.

Ambrose, R.J., Hartman, R.C., Campos, M.D., Akkutlu, I.Y., Sondergeld, C.H., 2010. New Pore-scale Considerations for Shale Gas in Place Calculations. Society of Petroleum Engineers, Paper SPE 131772, 17p.

Behar, F., Kressmann, S., Rudkiewicz, J.L., Vandenbroucke, M., 1992. Experimental simulation in a confined system and kinetic modelling of kerogen and oil cracking. Organic Geochemistry 19, 173–189.

Behar, F., Vandenbroucke, M., 1987. Chemical modelling of kerogens. Organic Geochemistry 11, 15–24.

Busch, A., Gensterblum, Y., Krooss, B.M., 2003. Methane and CO_2 sorption and desorption measurements on dry Argonne premium coals: pure components and mixtures. International Journal of Coal Geology 55, 205–224.

Bustin, R.M., Clarkson, C.R., 1998. Geological controls on coalbed methane reservoir capacity and gas content. International Journal of Coal Geology 38, 3–26.

Cavenati, S., Grande, C.A., Rodrigues, A.E., 2004. Adsorption equilibrium of methane, carbon dioxide and nitrogen on zeolite 13X at high pressures. Journal of Chemical Engineering Data 49, 1095–1101.

Chalmers, G.R.L., Bustin, R.M., 2007a. On the effects of petrographic composition on coalbed methane sorption. International Journal of Coal Geology 69, 288–304.

Chalmers, G.R.L., Bustin, R.M., 2007b. The organic matter distribution and methane capacity of the Lower Cretaceous strata of northeastern British Columbia, Canada. International Journal of Coal Geology 70, 223–239.

Clarkson, C.R., Bustin, R.M., 1996. Variation in micropore capacity and size distribution with composition in bituminous coal of the Western Canadian Basin. Fuel 75, 1483–1498.

Clarkson, C.R., Bustin, R.M., Levy, J.H., 1997. Adsorption of the mono/multilayer and adsorption potential theories to coal methane adsorption isotherms at elevated temperature and pressure. Carbon 35, 1689–1705.

Clarkson, C.R., Bustin, R.M., 1999. The effect of pore structure and gas pressure upon the transport properties of coal: a laboratory and modeling study. 1. Isotherms and pore volume distributions. Fuel 78, 1333–1344.

Clarkson, C.R., Bustin, R.M., 2000. Binary gas adsorption/desorption isotherms: effect of moisture and coal composition upon carbon dioxide selectivity over methane. International Journal of Coal Geology 42, 241–271.

Crosdale, P.J., Meamish, B.B., Valix, M., 1998. Coalbed methane sorption related to coal composition. International Journal of Coal Geology 35, 147–158.

Cui, X., Bustin, A.M., Bustin, R., 2009. Measurements of gas permeability and diffusivity of tight reservoir rocks: different approaches and their applications. Geofluids 9, 208–223.

Dubinin, M.M., 1975. Physical adsorption of gases and vapours in micropores. In: Cadenhead, D.A., Danielli, J.F., Rosenberg, M.D. (Eds.), Progress in Surface and Membrane Science, vol. 9. Academic Press, New York, pp. 1–70.

Düren, T., Sarkisov, L., Yaghi, O.M., Snurr, R.Q., 2004. Design of new materials for methane storage. Langmuir 20, 2683–2689.

Fathi, E., Akkutlu, I.Y., 2009. Matrix heterogeneity effects on gas transport and adsorption in coal bed and shale gas reservoirs. Journal of Transport in Porous Media 80, 281–304.

Goodman, A.L., Busch, A., Duffy, G.J., Fitzgerald, J.E., Gasem, K.A.M., Gensterblum, Y., Krooss, B.M., Levy, J., Ozdemir, E., Pan, Z., Robinson, R.L., Schroeder Jr., K., Sudibandriyo, M., White, C., 2004. An inter-laboratory comparison of CO_2 isotherms measured on Argonne premium coal samples. Energy and Fuels 18, 1175–1182.

Gregg, S.J., Sing, K.S.W., 1982. Adsorption, Surface Area and Porosity, second ed. Academic Press, New York.

Helgeson, H.C., Richard, L., McKenzie, W., Norton, D.L., Schmitt, A., 2009. A chemical and thermodynamic model of oil generation in hydrocarbon source rocks. Geochimica et Cosmochimica Acta 73, 594–695.

Hill, R.J., Jarvie, D.M., Zumberge, J., Henry, M., Pollastro, R.M., 2007. Oil and gas geochemistry and petroleum systems of the Fort Worth Basin. American Association of Petroleum Geologists Bulletin 91, 445–473.

Himeno, S., Komatsu, T., Fujita, S., 2005. High-pressure adsorption equilibria of methane and carbon dioxide on several activated carbons. Journal of Chemical Engineering Data 50, 369–376.

Jarvie, D.M., Hill, R.J., Ruble, T.E., Pollastro, R.M., 2007. Unconventional shale-gas systems: the Mississippian Barnett Shale of north central Texas as one model for thermogenic shale-gas assessment. In: Hill, R.J., Jarvie, D.M. (Eds.), Special Issue: Barnett Shale. American Association of Petroleum Geologists Bulletin, vol. 91, 475–499.

Joubert, J.I., Grein, C.T., Bienstock, D., 1974. Effect of moisture on the methane capacity of American coal. Fuel 53, 186–191.

Keller, J.U., Staudt, R., 2005. Gas Adsorption Equilibria: Experimental Methods and Adsorption Isotherms. Springer, New York, p. 422.

Krooss, B.M., van Bergen, F., Gensterblum, Y., Siemons, N., Pagnier, H.J.M., David, P., 2002. High pressure CH_4 and carbon dioxide adsorption on dry and moisture equilibrated Pennsylvanian coals. International Journal of Coal Geology 51, 69–92.

Lamberson, M.N., Bustin, R.M., 1993. Coalbed methane characteristics of Gates Formation coals, northeastern British Columbia: effect of maceral composition. American Association of Petroleum Geologists Bulletin 77, 2062–2076.

Levine, J.R., Johnson, P.W., Beamish, B.B., 1993. High pressure microgravimetry provides a viable alternative to volumetric method in gas sorption studies on coal. In: Proceedings of the 1993 International Coalbed Methane Symposium. University of Alabama, Tuscaloosa, pp. 187–195.

Li, D., Liu, Q., Weniger, P., Gensterblum, Y., Busch, A., Krooss, B.M., 2010. High-pressure sorption isotherms and sorption kinetics of CH_4 and CO_2 on coals. Fuel 89, 569–580.

Loucks, R.G., Reed, R.M., Ruppel, S.C., Jarvie, D.M., 2009. Morphology, genesis and distribution of nanometer-scale pores in siliceous mudstones of the Mississippian Barnett Shale. Journal of Sedimentary Research 79, 848–861.

Loucks, R.G., Ruppel, S.C., 2007. Mississippian Barnett Shale: lithofacies and depositional setting of a deep-water shale-gas succession in the Fort Worth Basin, Texas. American Association of Petroleum Geologists Bulletin 91, 579–601.

Lu, X.C., Li, F.C., Watson, A.T., 1995. Adsorption measurements in Devonian shales. Fuel 74, 599–603.

McCarty, R.D., Arp, V.D., 1990. A new wide range equation of state for helium. Advances in Cryogenic Engineering 35, 1465–1475.

Milliken, K.L., Rudnicki, M.D., Awwiller, D.N., 2012. Form and distribution of organic matter-hosted pores, Marcellus Formation (Devonian), Pennsylvania, USA. Third EAGE Shale Workshop, Shale Physics and Shale Chemistry: New Plays, New Science, New Possibilities, Barcelona, Spain, January, 2012.

Montgomery, S.L., Jarvie, D.M., Bowker, K.A., Pallastro, R.M., 2005. Mississippian Barnett Shale, Fort Worth basin, north-central Texas: gas-shale play with multi-trillion cubic foot potential. American Association of Petroleum Geologists Bulletin 89, 155–175.

Reed, R.M., Loucks, R.G., 2007. Imaging nanoscale pores in the Mississippian Barnett Shale of the northern Fort Worth Basin (abs). American Association of Petroleum Geologists, Annual Convention, Abstracts Volume 16, 115.

Ross, D.J.K., Bustin, R.M., 2007. Shale gas potential of the Lower Jurassic Gordondale Member, northeastern British Columbia, Canada. Bulletin of Canadian Petroleum Geology 55, 51–75.

Ross, D.J.K., Bustin, R.M., 2008. Characterizing the shale gas resource potential of Devonian-Mississippian strata in the Western Canada Sedimentary Basin: application of an integrated formation evaluation. American Association of Petroleum Geologists Bulletin 92, 87–125.

Ross, D.J.K., Bustin, R.M., 2009. The importance of shale composition and pore structure upon gas storage potential of shale gas reservoirs. Marine and Petroleum Geology 26, 916–927.

Rowe, H.D., Loucks, R.G., Ruppel, S.C., Rimmer, S.M., 2008. Mississippian Barnett Formation, Fort Worth Basin, Texas: bulk geochemical inferences and Mo-TOC constraints on the severity of hydrographic restriction. Chemical Geology 257, 16–25.

Ruppel, S.C., Loucks, R.G., 2008. Black mudrocks: lessons and questions from the Mississippian Barnett Shale in the southern Midcontinent. The Sedimentary Record 6, 4–8.

Ruppel, T.C., Grein, C.T., Bienstock, D., 1974. Adsorption of methane on dry coal at elevated pressure. Fuel 53, 152–162.

Setzmann, U., Wagner, W., Pruss, A., 1991. A new equation of state and tables of thermodynamic properties for methane covering the range from the melting line to 625 K at pressures up to 1000 MPa. Journal of Physical and Chemical Reference Data 20, 1061–1151.

Sondergeld, C.H., Ambrose, R.J., Rai, C.S., Moncrieff, J., 2010. Micro-structural Studies of Gas Shales. Society of Petroleum Engineers, Paper No. SPE 131771.

Strapoc, D., Mastalerz, M., Schimmelmann, A., Drobniak, A., Hasenmueller, N.R., 2010. Geochemical constraints on the origin and volume of gas in the New Albany Shale (Devonian–Mississippian), eastern Illinois Basin. American Association of Petroleum Geologists Bulletin 94, 1713–1740.

Tissot, B.P., Welte, D.H., 1984. Petroleum Formation and Occurrence, second ed. Springer-Verlag, New York.

Wang, F.P., Reed, R.M., 2009. Pore Networks and Fluid Flow in Gas Shales. Society of Petroleum Engineers, Paper No. SPE-124253, 8 p.

Xia, X., Litvinov, S., Muhler, M., 2006. A consistent approach to adsorption thermodynamics on heterogeneous surfaces using different empirical energy distribution model. Langmuir 22, 8063–8070.

Xia, X., Tang, Y., 2012. Isotope fractionation of methane during natural gas flow with coupled diffusion and adsorption/desorption. Geochimica et Cosmochimica Acta 77 (25), 489–503.